Chapter 5

Industrial Case Studies

Omne tulit punctum, qui miscuit utile dulci

5.1 General introduction

This chapter summarises the results obtained when applying the concepts and approaches developed in the two previous chapters to existing industrial cases studies. When considered appropriate, alternative approaches have been used as a reference in order to quantify the benefits achieved. This chapter illustrates how the developed strategies can be easily adapted and applied to existing industrial processes, thus complementing the benchmark examples previously considered. The first scenario contemplates the on-line optimisation of a continuous petrochemical process, while the second one, focuses in the optimisation of the semi-continuous operation of an evaporation station of a sugar cane production plant. Some original data and details have been deliberately withheld for confidentiality reasons, without compromising the validity of the results.

5.2 Industrial case study I: on-line optimisation of a paraffins separation plant

5.2.1 The process

The process consists in a train of two distillation columns where a mixture of paraffins is separated from kerosene (figure 5.1). The feed is a mix of hydrocarbons (paraffins containing significant quantities of aromatics, iso and cyclo-paraffins and some olefins) that is preheated in a heat exchanger (REC) which takes advantage of the energy of a lateral extraction of the Redistillation column (T-2). The light hydrocarbons (less than C-10) and sulphur are separated in the Stripper (T-1) at the top (Naphtha). The Stripper's bottom is fed to the Redistillation column, where the main product (Light) containing lineal hydrocarbons (C-10 to C-14) is obtained at the top and

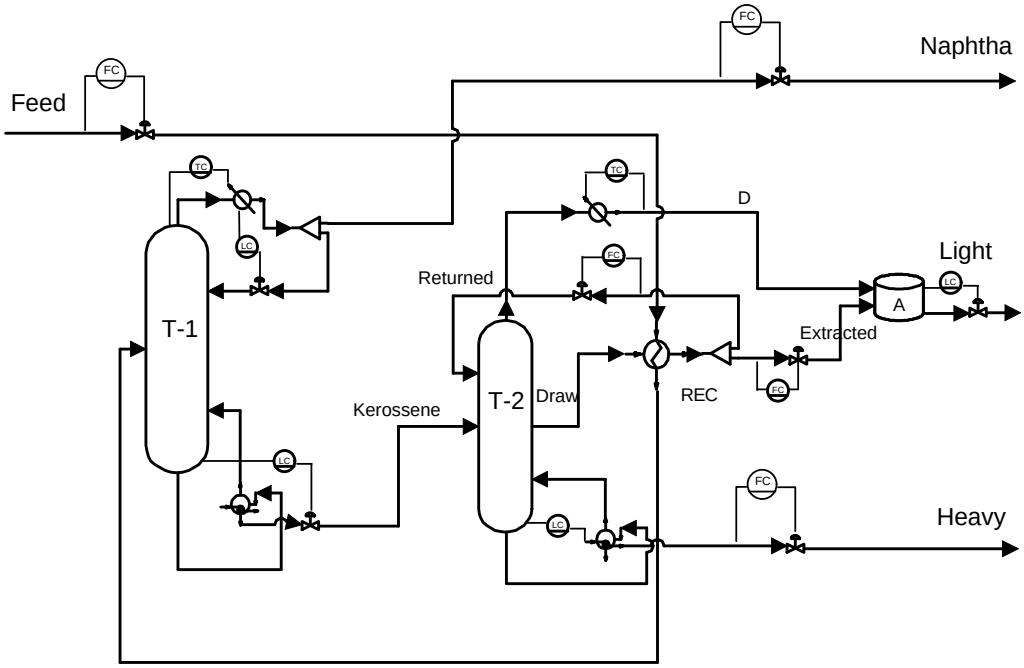

Figure 5.1: Simplified process flowsheet for the paraffins separation plant

heavy kerosene is obtained as by-product at the bottom. It is worth noting that the energy exchange between streams Feed and Draw results into a feedback, producing a strong interaction between both columns.

5.2.2 Steady state model

The steady state model has been developed using a sequential modular process simulator (Hysys.Plant). Data of five days of operation, sampled every five minutes related to the main variables (i.e. flows, temperatures, pressures, etc.) were used to adjust some parameters (tray efficiencies and the property package) until an acceptable accuracy of the process representation was obtained. The model has been conceived for process simulation given the main inputs given bellow:

- the *feed conditions*
  - flow (F_F)
  - temperature
  - pressure
  - composition
- and the following *specifications*

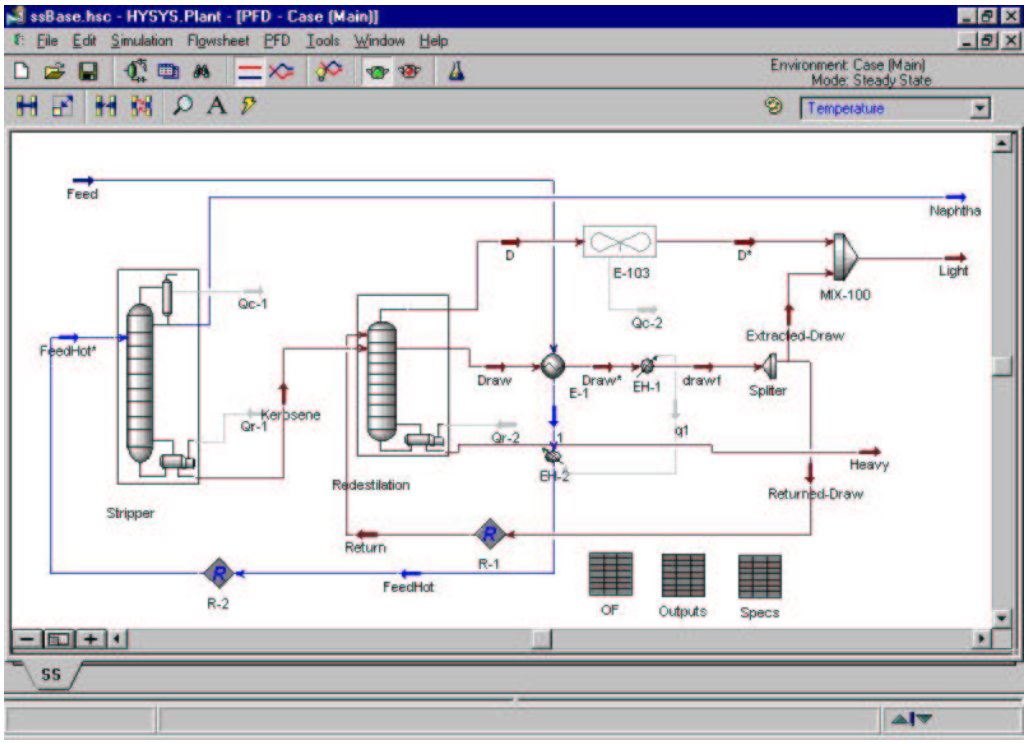

Figure 5.2: Screen-shot of the steady state model developed in Hysys.Plant

  - for the Stripper (T-1)
    - bottom and top pressures (assumed constants)
    - heat to reboiler ($Q_{h_{RebT1}}$)
  - for the Redistilation Column (T-2)
    - bottom and top pressures (assumed constants)
    - lateral extraction flow (F_{Draw})

- and finally, the split fraction corresponding to the draw extracted (Sf_E).

Additional "planning decision" specifications are the mass flow ratios of the three final products with respect to the feed. They are introduced as column specifications in T-1 (Naphtha) and T-2 (Heavy), while the last one (Light) is automatically satisfied to meet the global mass balance. Besides, there are other planning specifications related with product quality characterisation (API gravity index, Normal Boiling Point (NBP) and average molecular weight (MW)).

Figure 5.2 shows a screen-shot of the model developed. To properly simulate the process, two recycle blocks are required, indicated by the rhombus (R's). Two hypothetical heat exchangers (EH-1 and EH-2 in figure 5.2) are used to facilitate the simulation specification as well as to avoid an iterative calculation procedure in the heat exchanger REC. It should be mentioned that since they are not standard output parameters, the proper evaluation of the quality indicators

requires some programming effort, using the *user variable* capabilities of this flowsheeting software. In addition, in order to facilitate the data input-output and communication, three internal spreadsheets are used: one for introducing inputs and specifications, another for tabulating the key outputs and the remaining one to display the objective function related variables.

5.2.3 The performance model

The performance model describes the influence of operating conditions over the process economical and quality performance. Although the problem is multi-objective in nature, both aspects were aggregated in a single objective function. The instantaneous objective function (IOF), to be maximised is:

$$IOF = R - (H + C + RM) \tag{5.1}$$

where:

R: are the revenues obtained for selling the products (\$/h).

H: represents the heating costs (\$/h).

C: the cooling costs (\$/h).

RM: the raw material costs (\$/h).

Such terms are obtained by the addition of the individual contributions as follows:

$$R = \sum_j R_j \tag{5.2}$$

$$H = h_q \sum_j Q_{h_j} \tag{5.3}$$

$$C = c_q \sum_j Q_{c_j} \tag{5.4}$$

$$RM = r_m F_{rm} \tag{5.5}$$

where:

h_q, c_q and r_m are the corresponding economical weighting factors (\$/material or \$/energy).

F_{rm}: the raw material flow (material flow basis).

Q_h: denotes the energy associated to a heating stream (energy flow basis).

Q_c: denotes the energy associated to a cooling stream (energy flow basis).

j: denotes every element in the corresponding set.

In order to take into account the products quality, a quality index is computed using the quadratic difference between the nominal and the actual value of the quality-characterising parameter (*API*, *NBP* and *MW*), affecting the revenues term in penalising economic terms.

$$qf_{i,j} = \frac{(\kappa_{current_{i,j}} - \kappa_{nom_{i,j}})^2}{\kappa_{nom_{i,j}}} \tag{5.6}$$

where:

$qf_{i,j}$: is the quality index *i* for the product *j*.

$\kappa_{current_{i,j}}$: is the *actual* value of the quality parameter *i* for the product *j*.

$\kappa_{nom_{i,j}}$: is the *nominal* value of the quality parameter *i* for the product *j* (*planning specification*).

Therefore, the "pseudo" revenues obtained for the product *j* are computed using:

$$R_j = r_j \cdot F_{p_j} \cdot fq_j = r_j \cdot F_{p_j} \frac{1}{1 + \sum_j qf_{i,j} \cdot w_{i,j}} \quad \forall j \tag{5.7}$$

where:

F_{p_j}: is the product *j* flow (material flow basis).

r_j: is an economic conversion factor for the revenues of product *j* ($/material).

fq_j: is the global quality coefficient for the product *j* (dimensionless).

$w_{i,j}$: is a the weight coefficient for the pair quality-factor (*i*) - product (*j*), (dimensionless).

Thus, the selected *IOF* reflects the trade-off between energy consumption and product quality in a simplified way. It should be noted that although the objective function has the dimensions of *monetary units/time*, it must not be seen as a profit value because strictly speaking is an aggregated performance function.

5.2.4 Optimisation

The optimisation objective is to maximise the selected objective function, by modifying the specifications (decision variables) and observing a set of boundary constraints, for decision variables and product quality indexes. Besides, an additional operation constraint establishes that at least 20% of the light product should come directly form the tower T-2 (see stream D in the flowsheet of figure 5.1). This latter constraint has been used to link two of the decision variables in the form of an inequality as follows:
The mass balance in tank A gives:

$$F_L = F_D + Sf_E \cdot F_{Draw} \tag{5.8}$$

$$F_D = F_L - Sf_E \cdot F_{Draw} \tag{5.9}$$

then, as the constraint imposes:

$$F_D \geq 0.2 \cdot F_L \tag{5.10}$$

it is obtained:

$$Sf_E \geq 0.8 \cdot \beta_L \frac{F_F}{F_{Draw}} \tag{5.11}$$

where:

F_L: flow of the stream Light.

F_D: flow of the stream D.

F_F: flow of the stream Feed.

Sf_E: is the extracted split fraction.

β_L: is the ratio between the flows of streams Light and Feed (planning decision).

However, a sensitivity analysis indicates that this inequality (equation 5.11) is always active at the optimum point. Therefore, it has been explicitly included as an equation to reduce the degrees of freedom from three to two ($Q_{h_{RebT1}}$ and F_{Draw}). Both variables have been included as ratios to the current feed flow (F_F), to avoid non-desired variability to changes in the most frequent disturbance. Feed conditions are the main disturbances considered from the optimisation standpoint.

5.2.4.1 Off-line results

The base case (reference) corresponds to the nominal operating point, where the objective function has shown to be convex (figure 5.3). Additionally, the sensitivity of the optimal operating conditions has been evaluated off-line introducing variations on the feed conditions (i.e. see table 5.1). A pronounced change of the optimal operating point is found with the variability in feed temperature and composition.

5.2.4.2 On-line results

As shown by the scheme of the figure 3.9 (page 57) a dynamic first principles model is used to emulate “on line” data, which are consequently already validated, filtered and reconciled. The RT system includes the following components: the steady state detector used for model updating, the steady state process model and its associated performance model, the solver (in RTO is an optimisation algorithm while in RTE it is just the improvement algorithm) and finally the implementation block that sends the generated set-points to the plant, if they are acceptable.

Table 5.1: Off-line analysis

	Base case	*New* $(not-opt.)$	*New* $(opt.)$
Feed Conditions			
Flow (m3/h)	55.04	58.00	58.00
S* (%)	0.05	0.05	0.05
n-C8 to n-C10 (%)	6.00	5.89	5.89
n-C11-to n-C14 (%)	11.71	13.26	13.26
n-C15-to n-C17 (%)	1.26	1.24	1.24
Ciclo (%)	32.90	32.31	32.31
Iso (%)	28.00	27.51	27.50
Aromatics (%)	19.45	19.10	19.10
Ole (%)	0.67	0.65	0.65
Decision Variables			
$\frac{Q_{h_{RebT1}}}{F_F}$ (10^{-5} KJ/ m3 feed)	3.76	3.76	3.69
$\frac{F_{Draw}}{F_F}$ (m3/ 100 m3 feed)	61.10	61.10	51.80
Sf_E (m3/ 100 m3 draw)	77.25	77.25	90.00

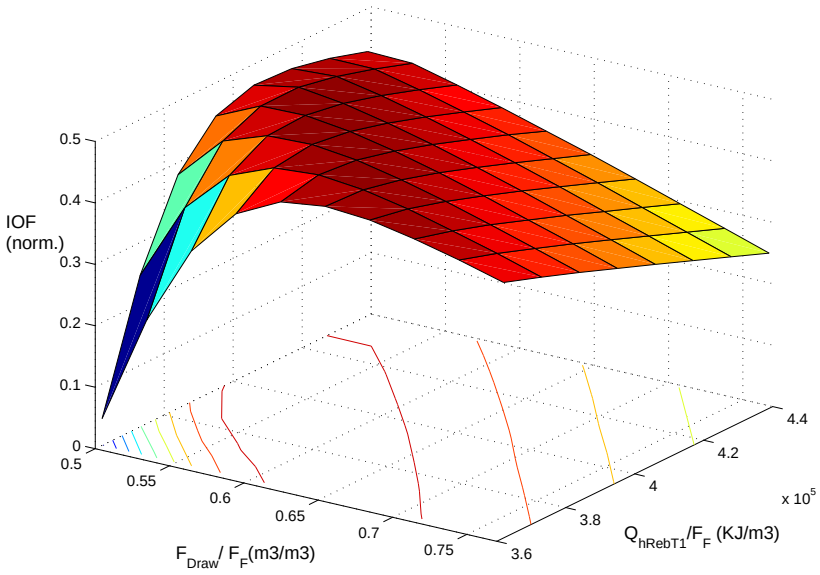

Figure 5.3: Sensitivity to decision variables

Table 5.2: Control scheme

Controller	Controlled variable	Manipulated Variable
General		
FC-Feed	Feed Flow	Feed Valve Opening
FC-Naphtha	Naphtha Flow	Naphtha Valve Opening
FC-Heavy	Heavy Flow	Naphtha Valve Opening
Tower T-1		
LC-Cond	Condenser Level	Reflux
TC-Top	Condenser Temperature	Heat from condenser
LC-Reb	Reboiler Level	Kerossene Flow
QC-Reb	Reboiler Heat flow	Heating Fluid Flow
Tower T-2		
LC-Reb	Reboiler Level	Heat to reboiler
TC-Top	Stream D temperature	Heat from condenser
FC-Returned	Returned Flow	Returned Valve Opening
FC-Extracted	Extracted Flow	Extracted Valve Opening

The dynamic model has been developed using Hysys.Plant, and for the communication with the RT system block the DCS interface has been used. It should be noted that the development of the dynamic model, besides a considerable degree of effort and expertise, requires the specification of a significant number of additional parameters, mainly related to the relationships between flow and pressure changes (an aspect rarely considered in steady state models although it is a potential source of plant-model mismatch).

The dynamic model includes the whole control layer. The control scheme is shown in table 5.2. All controllers are proportional-integral. For the sake of simplicity, some assumptions were made:

- perfect control for loop QC-Reb,
- perfect control for top pressures in both columns, using two vent streams in T-1 condenser and tank A,
- and perfect control for the heat exchanged in REC (QRec).

Such assumptions do not compromise the simulation results since the QC-Reb and QRec controllers have associated very fast dynamics. On the other hand, the columns pressures do not change substantially to include their variability in the model.

Figure 5.4 shows a screen-shot of such simulation, showing less than the half of the controllers required, what somehow illustrates the significant quantity of information to handle.

Several experiments have been performed using such model, simulating disturbances in input conditions and comparing the results obtained when using RTO and RTE, and when taking no optimising action. In the following, the case and results corresponding to a step change in compositions (10 % in average) and set-point of feed flow (5%) are commented.

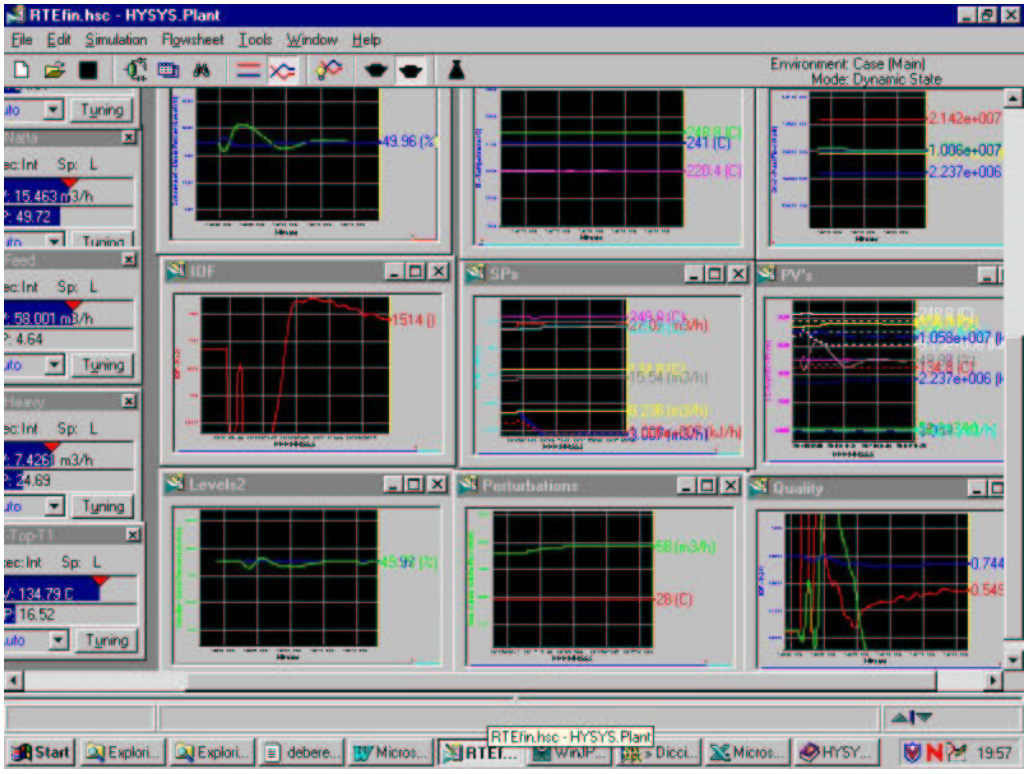

Figure 5.4: Screen-shot of the dynamic model

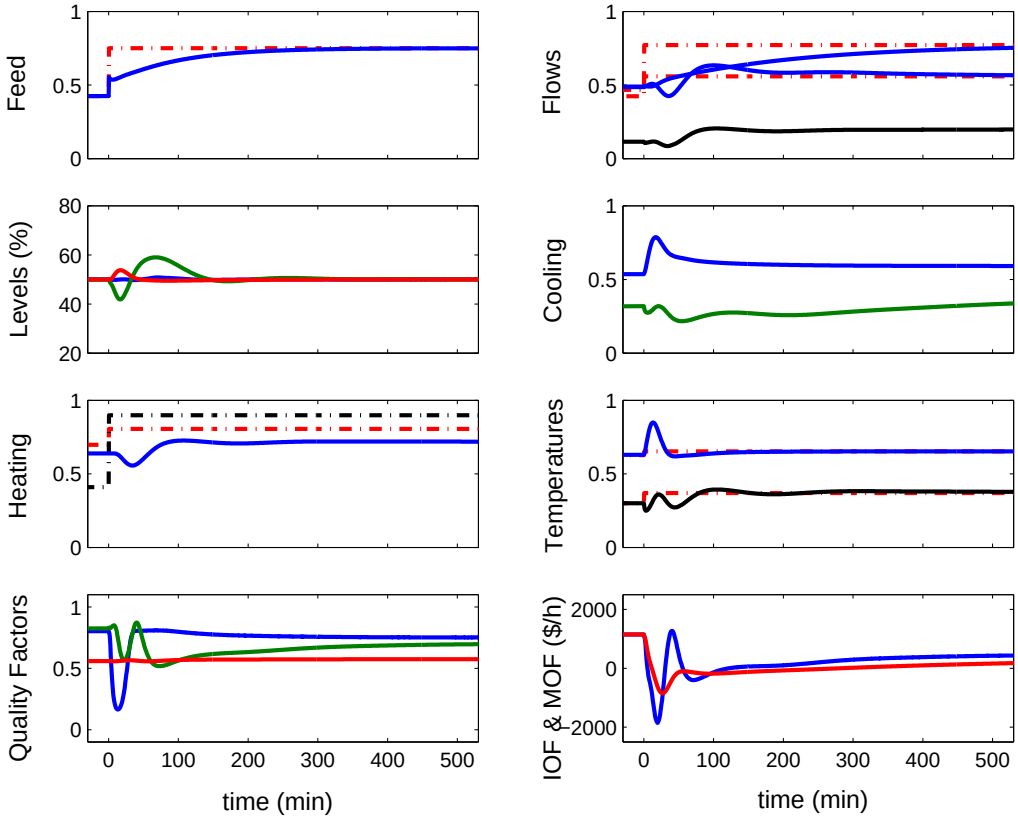

Figure 5.5: Without optimising action (set-points in dashed lines)

Without optimising action: this situation does not correspond to keeping every controller with a constant set-point. It corresponds to maintaining constant the decision variables values rather that the set-points. For this case study, the decision variables are related to the feed flow, and therefore the set-points for the controllers: QC-Reb (T-1), FC-Returned, FC-Extracted and the QRec will change proportionally to the feed flow in order to keep constant the decision variables ($Q_{h_{RebT1}}$, F_{Draw} and Sf_E). In practice, this situation is handled by the plant operators or more commonly by ratio controllers at the supervisory control level. The latter approach has been used during the simulations. The situation for the temperature controllers is similar, but in this case the model used to evaluate the set-point changes has been the same steady state model for optimisation instead of a ratio controller (e.g. a non-linear correlation).

Simulation results (figure 5.5) indicate that the system performance is reduced as a consequence of the disturbance, and that approximately after 200 minutes the system smoothly reaches the new steady state. As it can be seen, the process variables have been grouped by type and normalised when appropriate.

RTO: approximately after 200 minutes, the steady state is detected, and optimisation takes place. The resulting optimal operating point is implemented as a bounded step in the associated

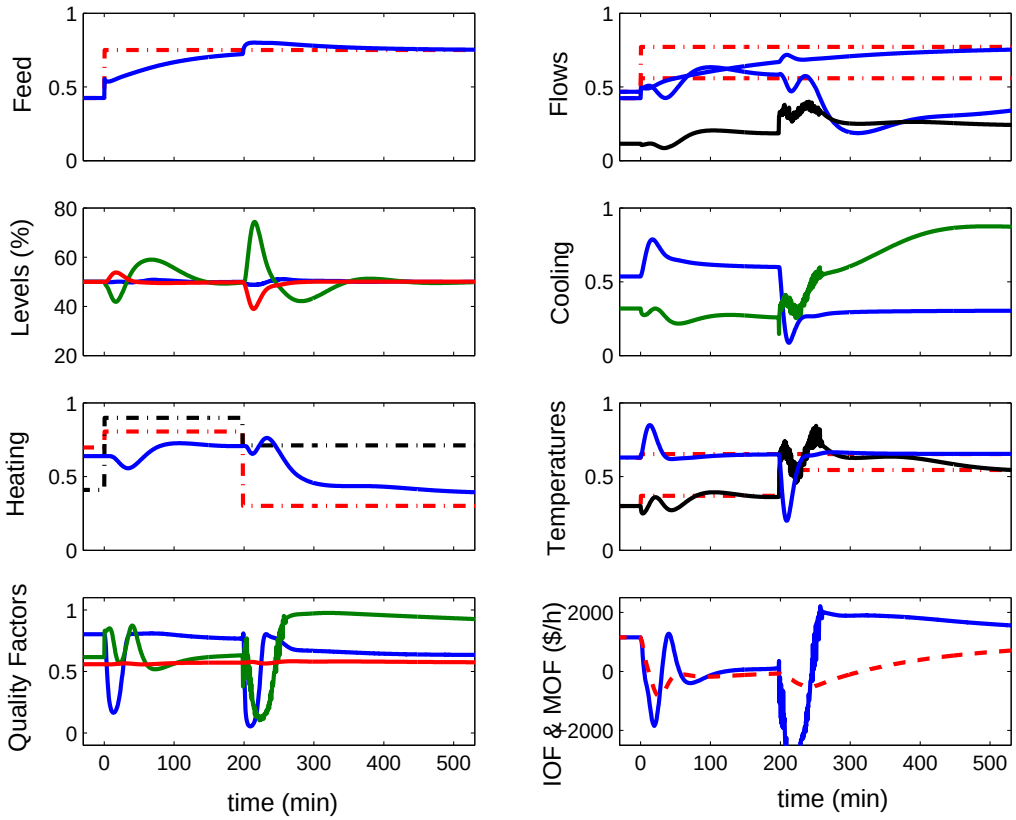

Figure 5.6: RTO

set-points (figure 5.6).

It is worth noting that the simultaneous implementation of set-points may produce a more significant system perturbation than the produced by the individual changes, besides the increase in the settling time (now about 400 min). An important consequence has been the appearance of small amount of vapor phase in some liquid streams, which compromise the performance of the corresponding flow controllers as have been seen in a noisy behaviour of some variables' curves. This fact imperatively suggests tightening the bounds associated to the set-point changes or improving the controllers' performance. Otherwise, the plant performance, in *IOF* terms, is substantially increased after 250 min.

RTE: RTE has been executed every 4 minutes, allowing a maximum decision variable change of 1%. Note that immediately after the disturbances occur (figure 5.7), the set-points are updated by the ratio controllers. Then, the system is progressively improving the operating points, (not necessarily by straight lines, as can be clearly seen in the charts for heating and temperatures). Besides, like in the RTO case, the process performance has been improved and an increase in the settling time can be also observed, although lower than that of the RTO case.

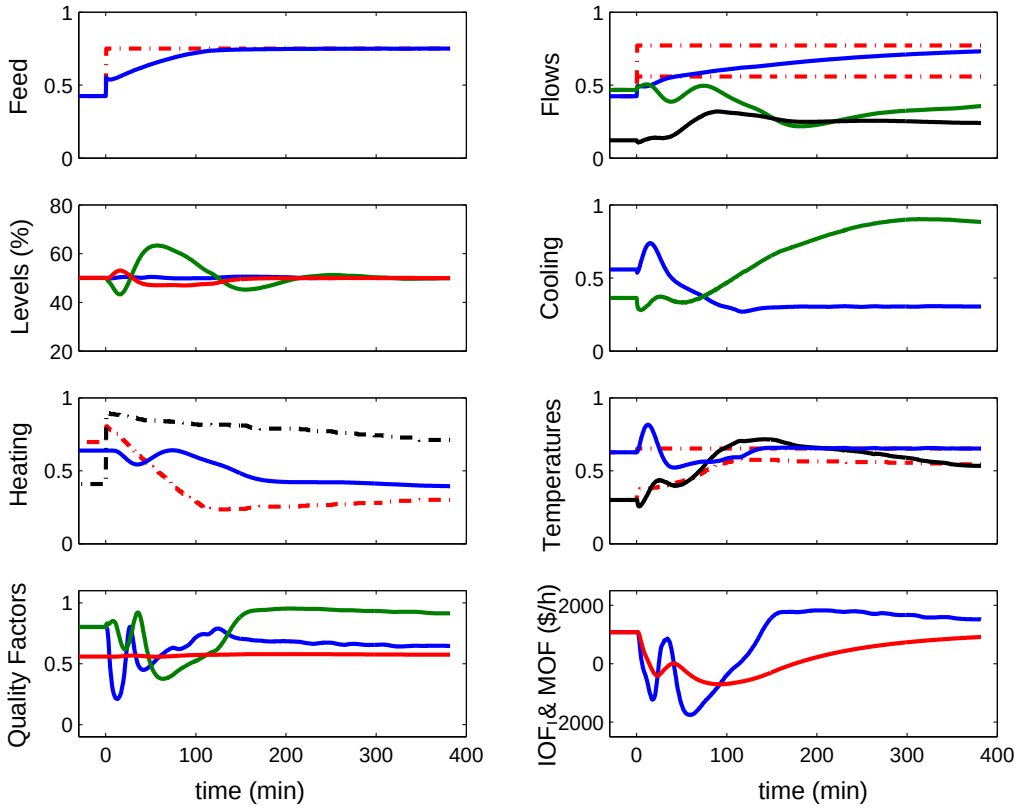

Figure 5.7: RTE

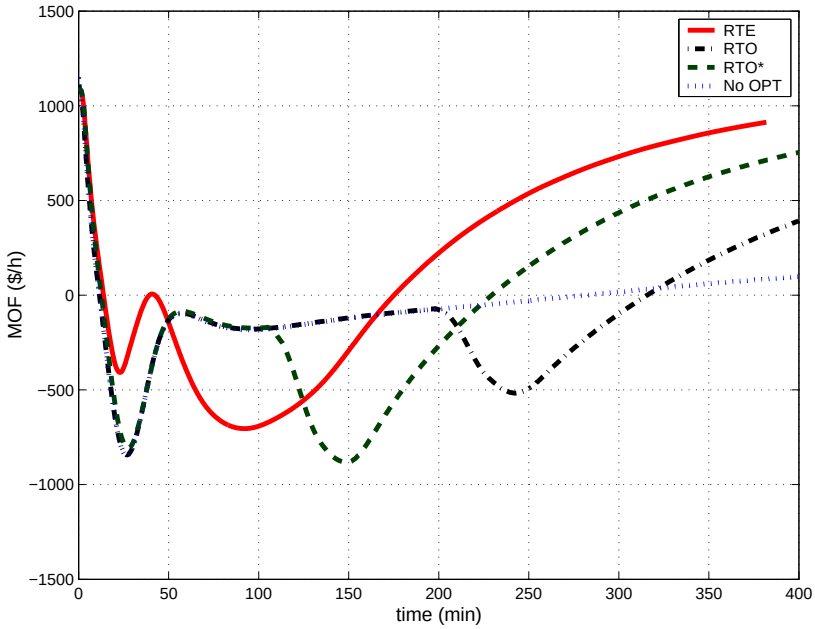

Figure 5.8: *MOF*'s

Final comments: figure 5.8 shows the Mean Objective Function (*MOF*), defined in section 3.3.1.1 (page 59) as:

$$MOF(t) = \frac{\int_{t_0}^{t} IOF(\theta)d\theta}{(t-t_0)} \tag{5.12}$$

(in other words, the mean performance during the interval $[t_0, t]$) for the three situations: without optimising action, RTO and RTE. It is clear that both RTE and RTO strategies improve the process performance as time goes by. However, the improvement produced by RTE is obtained sooner, thus making the system ready to deal with other disturbances without deteriorating the process performance. There is an additional curve in figure 5.8 describing the *MOF* behaviour for an RTO system with a less "strict" steady state detector (dashed line, RTO*). Although the process performance is improved faster, the minimum (in *MOF*) is more pronounced, which reveals a more aggressive behaviour of introducing a new disturbance when the system has not completely overcome the initial one.

5.2.5 Conclusions for the case study I

This section presents briefly some results obtained in the validation of an on-line optimisation system for an existing industrial scenario. The proposed validation scheme, involving dynamic simulation, gives a complementary vision of the system performance beyond the typical sensitivity and variability steady state analysis. Additionally, the simulations of the process do give insight into the problem, specifically, the fact of having a constraint always active (as mentioned

in the optimisation section) is by itself a bottleneck identification. This is greatly appreciated for process retrofitting purposes.

Furthermore, it has been illustrated how the corrective actions of an RT system introduce by themselves a disturbance on the system, which may compromise the process economical performance. Besides, it has been also shown the superior economical and operational behaviour of the RTE approach, in a real industrial scenario.

The system analysis has shown that the high degree of integration of the Stripper and Re-distillation columns makes the process transient too long, and therefore, an improved control strategy may help the use of on-line optimisation, becoming it more adequate and giving it the ability of coping with more frequent disturbances. Thus, an issue of major significance is that a re-engineering of the control layer is required for properly applying the classical RTO scheme. However, such re-engineering would not be required for implementing the RTE strategy, which proves again its simplicity and robustness and favour its industrial application.

5.3 Industrial case study II: planning of the cleaning tasks in a evaporation station

5.3.1 Process description

The sugar industry is the major source of incomes for many regions such as the northwest area of Argentina (Tucumán). A simplified flowsheet of a sugar factory there is shown in figure 5.9. The typical sugar process layout, consists of several mills in tandem after cane preparation with two sets of knives and using a compound imbibition of about 20-40% water on cane. Husks of sugar cane are sometimes used as fuel in the boilers. Clarification layout is conventional, with lime, sending the liquid cachaza from clarifiers to vacuum filters from where the filtrate is sent back to mixed juice before the addition of lime and the mud is used in agriculture as a fertiliser. Clarified juice with a solid concentration (Brix) 12 to 14 is sent from the clarifiers to the evaporation station, where it is concentrated to 61-64 Brix syrup.[1] Syrup is sent to the crystallisation section where it is processed.

The evaporation station is a source of motivation for optimisation since evaporation constitutes a critical stage for efficient management of water and energy resources. The vapour produced during the evaporation is used in many other sections of the plant for heating purposes. The aim of evaporation and crystallisation processes (see figure 5.10) of a sugar factory is to eliminate water from the juice and, thus, to obtain crystals of sucrose.

The evaporation process is economically more effective than the crystallisation process due to the multiple effect scheme. The water extracted from the juice by a n-effect scheme is approximately n times the steam used in the process. On the other hand, at the crystallisation stage the

[1] BRIX (degrees): unit divisions of the scale of a hydrometer, which, when placed in a pure aqueous sucrose solution at 20^{o}C, indicates the percentage by mass of dissolved solids in the solution. The reading obtained in an impure sucrose solution is usually accepted as an approximation of its percentage by mass of total soluble solids.

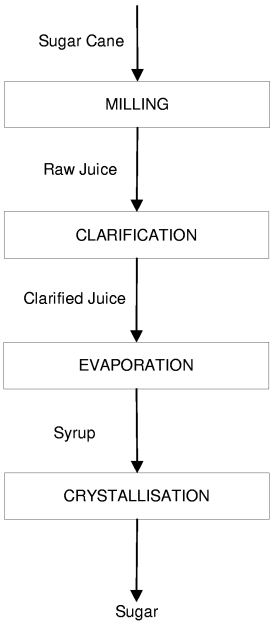

Figure 5.9: Simplified diagram of the sugar cane production process

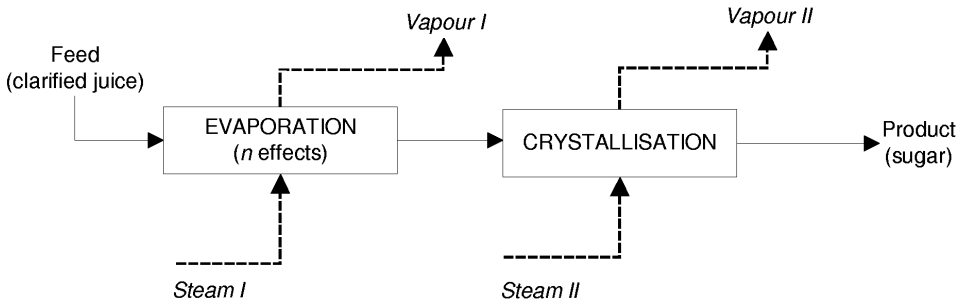

Figure 5.10: Efficiency of the steam usage

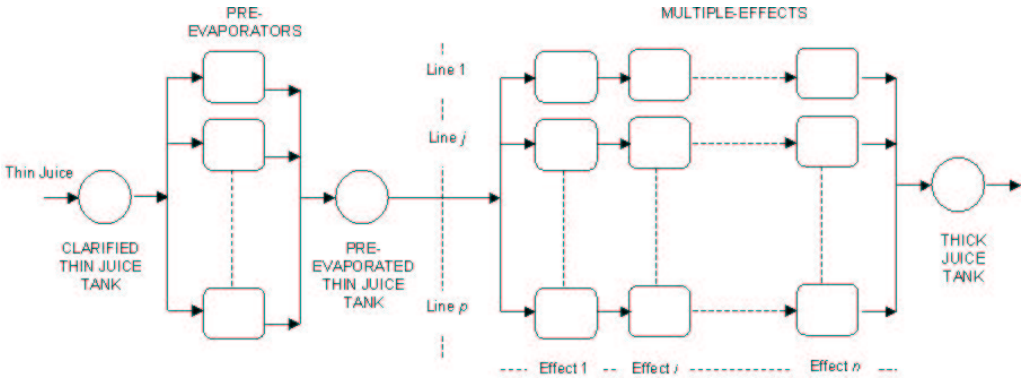

Figure 5.11: The evaporation station

water is extracted roughly in a proportion 1 : 1 with the consumed steam. Therefore, the minimum cost can be obtained maximising the outlet syrup sugar concentration from the evaporation station.

The evaporation process leads to the formation of fouling on the inner surface of the evaporator tubes. The rate of fouling formation is dependent on the nature of the feed, and is particularly significant for the case of liquid feeds. Fouling deposits inside the tubes act as insulation and offer higher heat-transfer resistance. It is necessary to periodically clean the equipment in order to restore conditions of higher heat-transfer rates. Thus, higher syrup concentrations require the evaporators to be cleaned frequently, which would decrease the production leading to a trade-off. This is a typical case of maintenance of units with decaying performance studied in chapter 4.

The evaporation station (figure 5.11) consists in two sequential stages. First, there is a pre-evaporation section that uses a single effect in each parallel line. The product is then sent to an intermediate storage tank, and fed to the parallel multiple-effects lines. The multiple-effects lines' products are send to another storage tank constituting the thick juice. The thick juice is latter processed in the crystallisers.

The operation optimisation problem can formally be stated in the following way.

- *Given:*
  - The amount of material to be processed.
  - The equipment models and parameters.
  - The individual equipment performances as time function.
- *Determine:*
  - The cleaning (maintenance) frequency.
  - The mass flow to be processed by each equipment.

And as explained before, the objective is to maximise the mean output sugar concentration at the outlet of the evaporation station.

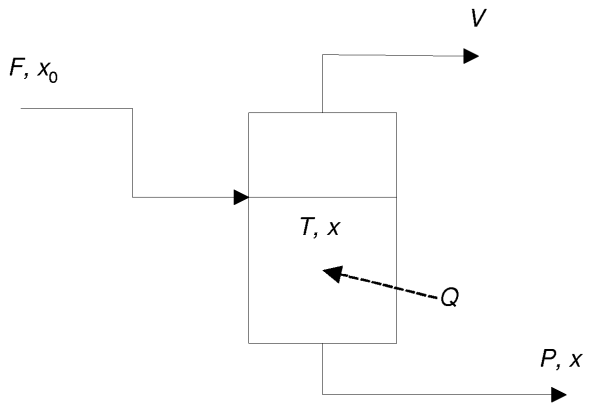

Figure 5.12: Single evaporator scheme

5.3.2 Off-line solution

5.3.2.1 A single evaporator

Consider a simple evaporator as illustrated in figure 5.12. A feed of sugar solution with a concentration X_0 arrives at a rate F.

The outlet concentration diminishes because of scaling over the outer sides of the evaporators' tubes, according to equation 5.13 (Honig, 1969):

$$U = \frac{a \cdot T}{X\sqrt{1 + b \cdot ts}} \tag{5.13}$$

where:

U: heat exchange coefficient ($\frac{Kcal}{h \cdot m^{2o}C}$)

T: liquid temperature (^oC)

X: product liquid concentration (% on weight basis)

a and b: parameters adjusted experimentally ($\frac{Kcal}{h \cdot m^{2o}C^2}$ and $\frac{1}{h}$ respectively)

For this case, the cleaning costs are negligible, and the objective is to find the time between cleaning operations in order to produce the maximum possible concentration during the cycle. The corresponding data for the specific problem are given in table 5.3.

Table 5.3: Data for a single evaporator

Variable	*Value*
$F\ (t/h)$	25
$T\ (^oC)$	103
$A\ (m^2)$	400
$\Delta T\ (^oC)$	13
$\lambda\ (\frac{Kcal}{kg})$	520
$a\ (\frac{Kcal}{h \cdot m^{2o}C^2})$	490
$\tau_m\ (h)$	14
$b\ (\frac{10^2}{h})$	2.77
$X_0\ (\%\, weight)$	12.00

The first step is to find $IOF(ts)$. Making the material and energy balances on pseudo stationary basis:
Material balance:

$$FX_0 = F_P X \tag{5.14}$$

$$F = F_V + F_P \tag{5.15}$$

Energy Balance:

$$Q \approx \lambda F_V \tag{5.16}$$

$$Q = UA \cdot \Delta T = \frac{aT}{X\sqrt{1+bts}} A \cdot \Delta T \tag{5.17}$$

where:

F_P: liquid product flow (*kg/h*).

F_V: vapour flow (*kg/h*).

λ: latent heat of steam (*kcal/kg*).

A: evaporator heat exchange area (m^2).

ΔT: temperature difference between steam and liquid (^oC).

Q: heat exchanged (*Kcal/h*).

Then:

$$IOF(ts) = X - X_0 = \frac{aTA \cdot \Delta T}{\lambda F\sqrt{1+bts}} \tag{5.18}$$

Since $IOF(ts_{opt}) = MOF(ts_{opt})$ (page 78):

$$\frac{aTA \cdot \Delta T}{\lambda F \sqrt{1+bts_{opt}}} = \frac{\frac{2aTA \cdot \Delta T}{b\lambda F}\left(\sqrt{1+bts_{opt}}-1\right)}{ts_{opt}+\tau_m} \tag{5.19}$$

or equivalently:

$$\frac{1}{\sqrt{1+bts_{opt}}} = \frac{\frac{2}{b}\left(\sqrt{1+bts_{opt}}-1\right)}{ts_{opt}+\tau_m} \tag{5.20}$$

Note that ts_{opt} only depends on b and τ_m and can be obtained in a recursive way, being ts_{opt} equal to 59 h for these conditions. That time corresponds to an average output concentration of 27,39% and a MOF of 12.44%. It should be also noted, that for this specific problem, the mean output sugar concentration during the whole cycle (X_m) is given by:

$$X_m = X_0 + MOF \tag{5.21}$$

while the relationship between MOF and the mean output concentration during the productive part of the cycle (the actual one) is given by:

$$X_p = X_0 + MOF\frac{ts+\tau_m}{ts} \tag{5.22}$$

An important issue is that the feed has been considered constant during the previous optimisation. Although the results can be improved by considering its temporal profile as a decision variable, the tight production conditions and mainly the associated storage requirements make such possibility impracticable, as indicated by plant personnel.

5.3.2.2 Parallel units in the pre-evaporation section

As for the single unit problem, the idea is to obtain the product with the maximum possible concentration. To compute the concentration at the outlet of the pre-evaporation section, the overall mass balances can be used:
Total mass of sugar produced (MX_T):

$$MX_T = \sum_j F_{P_j} X_{p_j} \frac{ts_j+\tau_{m_j}}{ts_j} \tag{5.23}$$

Total product mass (M_T):

$$M_T = \sum_j F_{P_j} \frac{ts_j+\tau_{m_j}}{ts_j} \tag{5.24}$$

then:

$$\overline{X} = \frac{MX_T}{M_T} = \frac{\sum_j F_{P_j} X_{p_j} \frac{ts_j+\tau_{m_j}}{ts_j}}{\sum_j F_{P_j} \frac{ts_j+\tau_{m_j}}{ts_j}} = \sum_j P f_j X_{p_j} \tag{5.25}$$

where $Pf_j = \frac{F_{P_j}\frac{ts_j+\tau_{m_j}}{ts_j}}{\sum_j F_{P_j}\frac{ts_j+\tau_{m_j}}{ts_j}}$ denotes the fractional production associated to the line j.

The terms $\frac{ts_j+\tau_{m_j}}{ts_j}$ are required to take into account the existence of the non-producing part of the sub-cycle. A more convenient expression for the objective function can be obtained using the following transformation:
Adding and subtracting X_0 and noting that $\sum_j Pf_j = 1$:

$$\overline{X} = X_0 + \sum_j Pf_j(X_{p_j} - X_0) \tag{5.26}$$

Multiplying and dividing every term of the summation by $\frac{ts_j+\tau_{m_j}}{ts_j}$:

$$\begin{aligned} \overline{X} = X_0 + \textstyle\sum_j Pf_j \frac{ts_j+\tau_{m_j}}{ts_j}(X_{p_j} - X_0)\frac{ts_j}{ts_j+\tau_{m_j}} = \\ = X_0 + \textstyle\sum_j Pf_j' \cdot MOF_j = X_0 + Z \end{aligned} \tag{5.27}$$

Considering besides that X_0 is constant, $max\,\overline{X} = max\,Z$. Therefore, the problem can be stated considering as decision variables the sub-cycle times ts_j for every unit j and the feed fractions to every line, Ff_j. Therefore, using the concepts introduced before, a possible problem formulation (*MP1*) is as follows:

$$\begin{aligned} \underset{ts_j, Ff_j}{max\,Z} \quad &= \textstyle\sum_j MOF_j(ts_j, Ff_j) \cdot Pf_j'(ts_j, Ff_j) \end{aligned} \tag{5.28}$$

subject to:

$$MOF_j = \frac{\frac{2a_jT_jA_j\cdot\Delta T_j}{b_j\lambda F f_j F_T}\left(\sqrt{1+b_jts_j}-1\right)}{ts_j+\tau_{m_j}} \quad \forall j \tag{5.29}$$

$$Ff_j = \frac{F_{m_j}}{F_T} \quad \forall j \tag{5.30}$$

$$\sum_j Ff_j = 1 \tag{5.31}$$

$$X_{p_j} - X_0 = MOF_j\frac{ts_j+\tau_{m_j}}{ts_j} \quad \forall j \tag{5.32}$$

$$Pf_j' = \frac{Ff_j\frac{X_0}{X_{p_j}}}{\sum_k Ff_k\frac{X_0}{X_{p_k}}}\frac{ts_j+\tau_{m_j}}{ts_j} \quad \forall j \tag{5.33}$$

$$F_{lo_j} \le F_{m_j}\frac{ts_j+\tau_{m_j}}{ts_j} \le F_{up_j} \quad \forall j \tag{5.34}$$

where:

$Pf_j' = Pf_j\frac{ts_j+\tau_{m_j}}{ts_j}$ denotes the fraction of product produced by unit j, being a function of the

Table 5.4: Data for the pre-evaporation section

Parameter	A	B	C	D	E
$F_{lo}\ (t/h)$	10	8	8	10	8
$F_{up}\ (t/h)$	40	28	28	40	28
$T\ (^oC)$	103	103	103	103	103
$A\ (m^2)$	400	350	350	400	350
$\Delta T\ (^oC)$	13	13	13	13	13
$\lambda\ (\frac{Kcal}{kg})$	520	520	520	520	520
$a\ (\frac{Kcal}{h \cdot m^{2o}C^2})$	490	490	490	490	490
$\tau_m\ (h)$	14	12	12	14	12
$b\ (\frac{10^2}{h})$	2.77	2.77	2.77	2.77	2.77
$X_0\ (\%\, weight)$	12.00				
$F_T\ (t/h)$	100				

decision variables Ff_j and ts_j.

Ff_j: denotes the fraction of feed devoted to unit j, being a decision variable.

F_{m_j}: average feed flow rate to unit j during the whole sub-cycle (*kg/h*).

F_{lo_j}: lower bound in F_j value (*kg/h*).

F_{up_j}: lower bound in F_j value (*kg/h*).

F_T: mass flow of the solution arriving to the evaporation station (*kg/h*).

And the remaining variables keep their previous meanings. In other words, the contribution to the global system *MOF* (termed Z) is proportional to the production output ($Pf_j^{'}$). The constraints are just the mass balances and the *MOF* definition. The corresponding data are given in table 5.4.

Although the solution of the mathematical problem (*MP1*) allows to obtain the optimum, the problem can be significantly simplified by using the equation 5.19 and the concepts of section 5.3.2.1 (page 117) to obtain the set of individual optimal sub-cycle times. This allows reducing the decision variables number to a half.

Additionally, note that for the example considered, the parameters for evaporators A and D are the same and so they are for the subset B, C and E. Therefore $Ff_A = Ff_D$ and $Ff_C = Ff_E = Ff_B$, then the problem complexity can be reduced again. Furthermore, as $\sum_j Ff_j = 1$ from equation 5.31, it remains only one degree of freedom.

In this way, using Ff_A as independent variable, it is possible to obtain the optimal conditions, as illustrated in the figure 5.13. The associated results are summarised in table 5.5.

Exactly the same solution is obtained by solving the whole formulation *MP1* using CONOPT2, in the GAMS modelling environment. Although the problem has several non-linearities, the solution obtained has shown no dependence on the starting point. It takes between

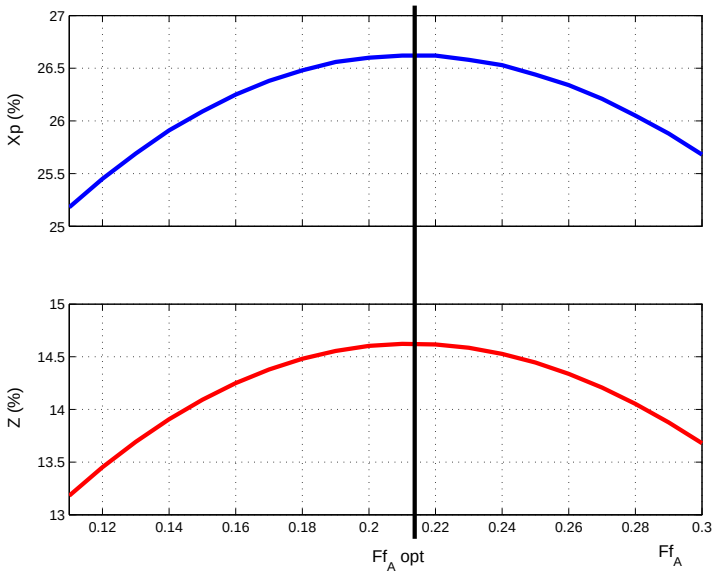

Figure 5.13: Pre-evaporation section solution

Table 5.5: Pre-evaporation section solution

Decision Variables	*A*	*B*	*C*	*D*	*E*
$Ff\ (\%)$	21.27	19.15	19.15	21.27	19.15
$ts\ (h)$	58.96	53.62	53.62	58.96	53.62
Other Variables					
$Pf\ (\%)$	26.32	23.44	23.44	26.32	23.44
$X_p\ (\%)$	26.62	26.62	26.62	26.62	26.62
$MOF\ (\%)$	11.82	11.95	11.95	11.82	11.95
$Z\ (\%)$	14.62				
$\overline{X}\ (\%)$	26.62				

0.1 and 0.5 seconds to solve every problem.[2]

In order to illustrate the benefits obtained using the proposed formulation, consider a single heuristic rule that is not far from the current operating way: the evaporators are cleaned twice per week ($ts = 72\,h$), and all of them consume the same quantity of feed ($Ff = 25\,\%$). Such solution corresponds to an average output concentration of 23.60%. Therefore the relative improvement obtained is about 11%. An alternative formulation (*MP2*), stated similarly to that of Jain and Grossmann (1998), is included in the appendix D (page 197) to illustrate the lower complexity and higher efficiency of the proposed approach.

5.3.2.3 Parallel multiple-effect lines

In order to apply the previous formulation to the specific problem, the model for *MOF* is needed, and it is obtained as follows:

Preliminary calculations: first, the instantaneous output concentrations and outflow are computed for every line j ($j = 1 \dots p$) using the equation 5.18 as follows:

$$X_{1,j} = X_0 + \frac{\beta_{1,j}}{F_{0,j}\sqrt{1 + b_j ts_j}} \quad \forall j \tag{5.35}$$

$$X_{2,j} = X_0 + \frac{\beta_{1,j}}{F_{0,j}\sqrt{1 + b_j ts_j}} + \frac{\beta_{2,j}\left(X_0 + \frac{\beta_{1,j}}{F_{0,j}\sqrt{1+b_j ts_j}}\right)}{F_{0,j}\sqrt{1 + b_j ts_j}} \quad \forall j \tag{5.36}$$

So that:

$$X_{i,j} = X_{i-1,j} + \frac{\beta_{i,j} X_{i-1,j}}{F_{0,j} X_0 \sqrt{1 + b_j ts_j}} = X_0 \prod_{k=1}^{i} \left(1 + \frac{\beta_{k,j}}{F_{0,j} X_0 \sqrt{1 + b_j ts_j}}\right) \quad \forall i, j \tag{5.37}$$

$$F_{i,j} = \frac{F_{0,j} X_0}{X_{i,j}} = \quad \forall i, j \tag{5.38}$$

where:

$$\beta_{i,j} = \frac{a_{i,j} T_{i.j} A_{i,j} \cdot \Delta T_{i,j}}{\lambda} \quad \forall i, j \tag{5.39}$$

and $i = 1 \dots n$ denotes the effect. Therefore, next step involves the calculation of the Instantaneous Objective Function (IOF_j) for every line, that is to say, the difference between the output (of the last effect n) and input sugar concentrations:

$$IOF_j = X_{n,j} - X_0 \tag{5.40}$$

[2] Using a AMD-K7 processor with 128 Mb RAM at 600 MHz, while about 2 seconds in an spreadsheet environment using an implementation of GRG2.

Using equation 5.37 it can be obtained:

$$IOF_j = \sum_{i=1}^{n} \frac{S_{i,j}}{F_{0,j}(F_{0,j}X_{0.j})^{i-1}(1+b_j ts_j)^{\frac{i}{2}}} \tag{5.41}$$

where the coefficients $S_{i,j}$ are computed using:

$$\begin{array}{rcll} S_{1,j} & = & \sum_{i=1}^{n} \beta_{i,j} & \\ S_{2,j} & = & \sum_{i=1}^{n} \sum_{r=i+1}^{n} \beta_{i,j}\beta_{r,j} & \\ S_{3,j} & = & \sum_{i=1}^{n} \sum_{r=i+1}^{n} \sum_{s=r+1}^{n} \beta_{i,j}\beta_{r,j}\beta_{s,j} & \forall j \\ S_{4,j} & = & \sum_{i=1}^{n} \sum_{r=i+1}^{n} \sum_{s=r+1}^{n} \sum_{t=s+1}^{n} \beta_{i,j}\beta_{r,j}\beta_{s,j}\beta_{t,j} & \\ S_{5,j} & = & \sum_{i=1}^{n} \sum_{r=i+1}^{n} \sum_{s=r+1}^{n} \sum_{t=s+1}^{n} \sum_{u=t+1}^{n} \beta_{i,j}\beta_{r,j}\beta_{s,j}\beta_{t,j}\beta_{u,j} = \prod_{i=1}^{n} \beta_{i,j} & \end{array} \tag{5.42}$$

The *MOF* expression: integrating the previous expression according to:

$$MOF_j = \frac{\int_0^{ts_{i,j}} [X_{n,j}(\theta) - X_0]\, d\theta}{ts_j + \tau_{m_j}} \quad \forall j \tag{5.43}$$

allows the evaluation of the Mean Objective Function during every sub-cycle for every line j. Assuming the same $b_{i,j}$ coefficient for every effect i, the following equation is obtained:

$$MOF_j = \sum_{i=1 \wedge i \neq 2}^{n} \frac{\left(\frac{2}{i-2}\right) S_{i,j} \left[\left(1+b_j ts_j\right)^{\left(\frac{i-2}{2}\right)} - 1 \right]}{F_{0,j}(F_{0,j}X_{0.j})^{i-1} b_j (ts_j + \tau_{m_j}) \left(1+b_j ts_j\right)^{\left(\frac{i-2}{2}\right)}} + \\ + \frac{S_{2,j} \ln(1+b_j ts_j)}{F_{0,j}(F_{0,j}X_{0.j}) b_j (ts_j + \tau_{m_j})} \qquad \forall j \tag{5.44}$$

It should be noted that for $n = 1$ such equation is equivalent to the equation 5.29.

Solution: once obtained the expression for *MOF*, it can be included in *MP1* and solve the multiple-effects lines problem using the data given in table 5.6 ($n = 5$, $p = 5$).

The solution obtained, which is given in the table 5.7, corresponds to an objective function value of 35.37%, equivalent to an overall mean output sugar concentration of 61.98%.

The solution has been obtained by solving the whole formulation *MP1* using CONOPT2, in the GAMS modeling environment. Although the problem has also several non-linearities, as in the case of parallel units, the solution obtained has shown no dependence on the starting points (200 starting points, randomly selected using a uniform distribution have been used).[3]

It should be noted that the dependence of ts_{opt} with Ff makes not possible the application of the simplified procedure used for solving the pre-evaporation section problem.

[3]It takes between 0.1 and 0.3 seconds to solve every problem in an AMD-K7 processor with 128 Mb RAM at 600 MHz, while about 1.5 seconds in an spreadsheet environment using an implementation of GRG2.

Table 5.6: Data for the multiple-effects lines section

Parameter	*A*	*B*	*C*	*D*	*E*
$F_{lo}\ (t/h)$	5	4	4	5	4
$F_{up}\ (t/h)$	20	14	14	20	14
$\tau_m\ (h)$	14	12	12	14	12
$a\ (\frac{Kcal}{h \cdot m^2 {}^oC^2})$	490	490	490	490	490
$\lambda\ (\frac{Kcal}{kg})$	520	520	520	520	520
$b\ (\frac{10^2}{h})$	2.77	2.77	2.77	2.77	2.77
$X_0\ (\%\, weight)$	26.62				
$F_T\ (t/h)$	50				
Coefficients $\beta_{i,j}\ (kg/h)$					
$\beta_{1,j}$	841	736	736	841	736
$\beta_{2,j}$	841	736	736	841	736
$\beta_{3,j}$	841	736	736	841	736
$\beta_{4,j}$	841	736	736	841	736
$\beta_{5,j}$	841	736	736	841	736

Table 5.7: Multiple-effect lines section solution

Decision Variables	*A*	*B*	*C*	*D*	*E*
Ff (%)	21.27	19.16	19.16	21.27	19.16
$ts\,(h)$	60.88	55.25	55.25	60.88	55.25
Other Variables					
Pf (%)	26.15	23.32	23.32	26.15	23.32
X_p *(%)*	62.00	61.97	61.97	62.00	61.97
MOF (%)	28.77	29.04	29.04	28.77	29.04
Z (%)	35.36				
$\overline{X}$ *(%)*	61.98				

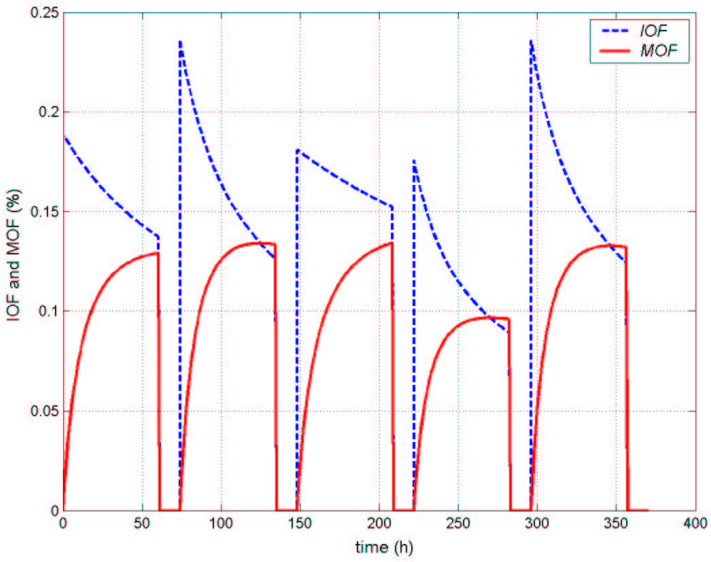

Figure 5.14: Strict implementation of off-line results

5.3.3 On-line Approach

Consider the simplest situation, with only one evaporator, where the off-line optimal solution for the available data corresponds to $ts = 59\,h$. The strict implementation of this result over a dynamic simulation (Aspen Custom Modeler, AspenTech (1998)) including variability and plant-model mismatch is shown in figure 5.14.

However, a system which determines ts_{opt} on line according to the proposed strategy leads to better performance when model mismatch and variability are present (figure 5.15). This is of special interest for this particular problem, given the significant presence of plat-model mismatch and what is even more pronounced, the cycle-to-cycle variability. Furthermore, the pseudo steady-state assumption has also its limitations, as it is shown in appendix E (page 201).

As explained in section 4.4 (page 87) on-line determination of the optimality condition (i.e $IOF = MOF$, according to the equation 5.19) may not necessarily lead to the same ts_{opt} value obtained off-line.

Strictly off-line and on-line approaches were thus compared via Monte Carlo simulation, by modelling the empirical parameters a and b using equation 4.40 as in chapter 4. Figure 5.16 shows the resulting distribution of the actual ts_{opt} obtained for $\sigma = 10\,\%$ and $\xi = 10\,\%$, where the value obtained for ts, according to the off-line procedure, is included as a reference.

A larger set of Monte Carlo simulations for different values of σ and ξ leads to the results shown in figure 5.17. The difference between the performances (MOF) of both approaches is again used as comparative index.

As expected, the on-line determination of ts_{opt} enhances the process performance. For this

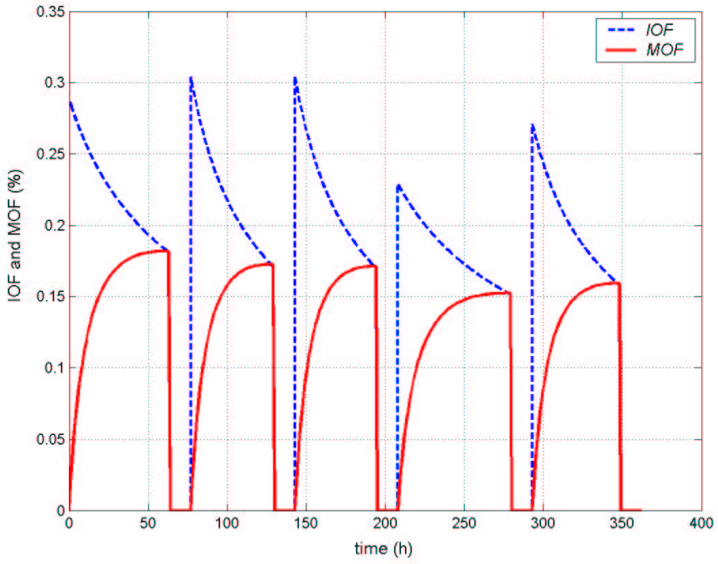

Figure 5.15: On-line approach

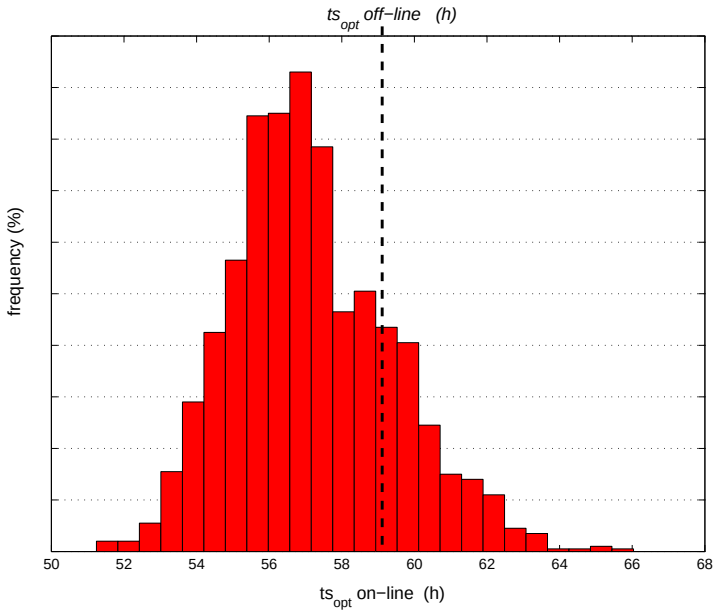

Figure 5.16: Histogram of ts_{opt} distribution for $\sigma = 10\,\%$ and $\xi = 10\,\%$

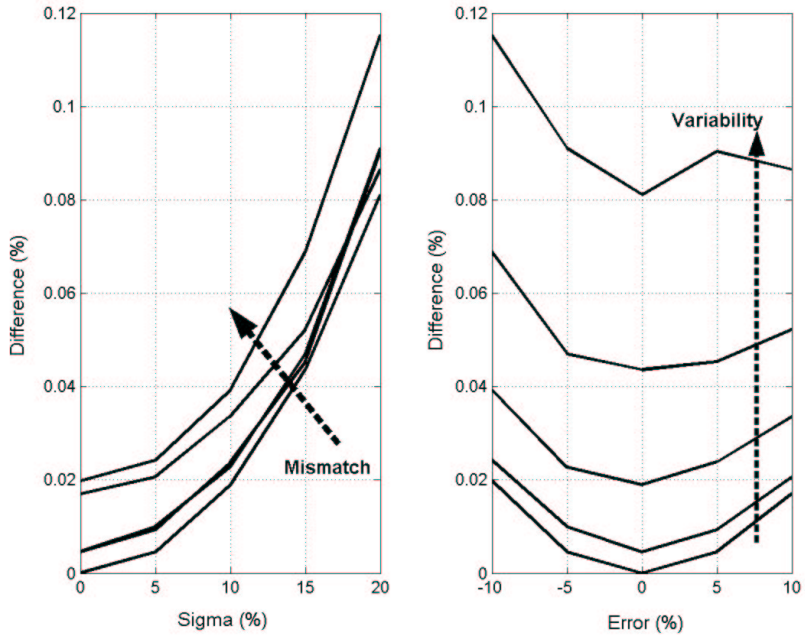

Figure 5.17: Improvement obtained using RTE for different variability and plant-model mismatch conditions

particular example, the approximated improvement is about 0.11% in terms of concentration, in absolute terms and according to the given flow-rate, corresponds to more than 200 *tn-sugar/year*. Considering that usually the evaporation station involves several equipments (figure 5.11), the on-line determination of cleaning tasks may be greatly compensated.

To clarify the extension to the remaining system, consider the pre-evaporation section. Once solved the off-line problem, the assignment of feeds to be processed to every parallel equipment has been already made. Therefore, the presented procedure for on-line optimisation (the same that for a single equipment) can be readily used to determine the optimal sub-cycle times on-line, reducing thus the plant-model mismatch as well the variability effects. For such case, the strategy is given in the algorithm 3.

Such procedure is equivalent for any number of multiple effect evaporators, because once assigned the corresponding feed flow, the individual behaviour corresponds to that of the simplest case.

Regarding the operational constraints in F, it should be noted that although ts is determined on-line, it will be bounded in order to observe F_{lo} and F_{up} related constraints. Consider for instance that according to the off-line results, the Ff values are decided. The feed to every line will be:

$$F_j = Ff_j \cdot F_T \cdot \frac{(ts_j + \tau_{m_j})}{ts_j} \quad \forall j \tag{5.45}$$

Algorithm 3 Procedure for the parallel units (or lines)

Initialisation
Solve the problem off-line to obtain
an estimation for F and ts (Ff is fixed)
Main loop
Do (for every line)
  Assign F (as set-points to ratio to feed flow rate controllers)
  Do
    Monitor plant and continuously forecast ts
  Until ts satisfies $\frac{dMOF}{dts} = 0$ (on-line)
  Perform the cleaning task
  Update mean ts estimation using
  $ts_{k+1} = ts_k \cdot \alpha + ts_{k-1} \cdot (1-\alpha)$ with $0 \leq \alpha \leq 1$
  (damping factor).
  Update F to keep Ff using $F = Ff \cdot F_T \cdot \frac{(ts+\tau_m)}{ts}$
  $k \leftarrow k+1$
Until new off-line solution

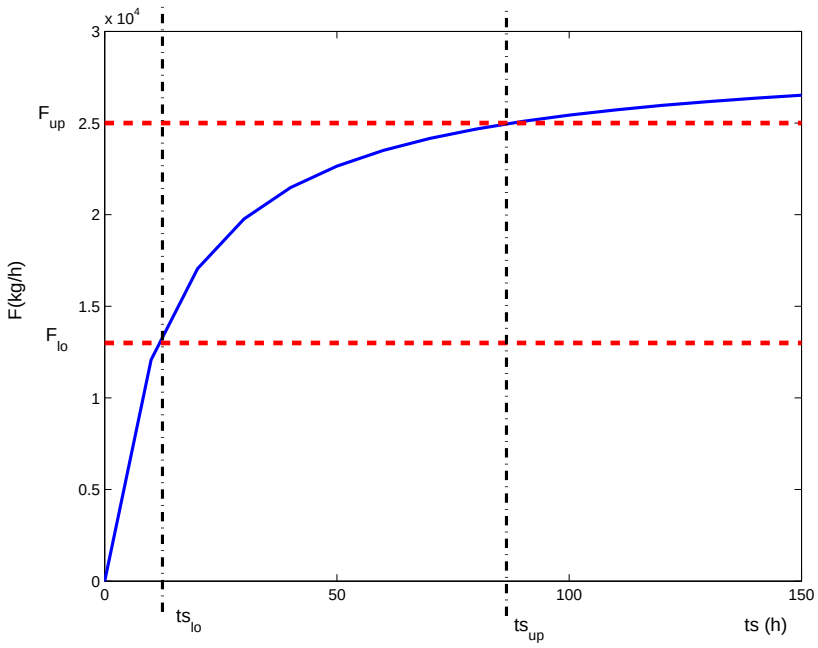

Figure 5.18: Bounds in ts

Therefore, for a given input flow rate (F_T) and decided feed fractions ($Ff_j's$), the corresponding feed flows ($F_j's$) will have the bounds as shown in figure 5.18. Consequently, the on-line procedure (for the line j) must not be active for the corresponding range of ts_j that make infeasible F_j.

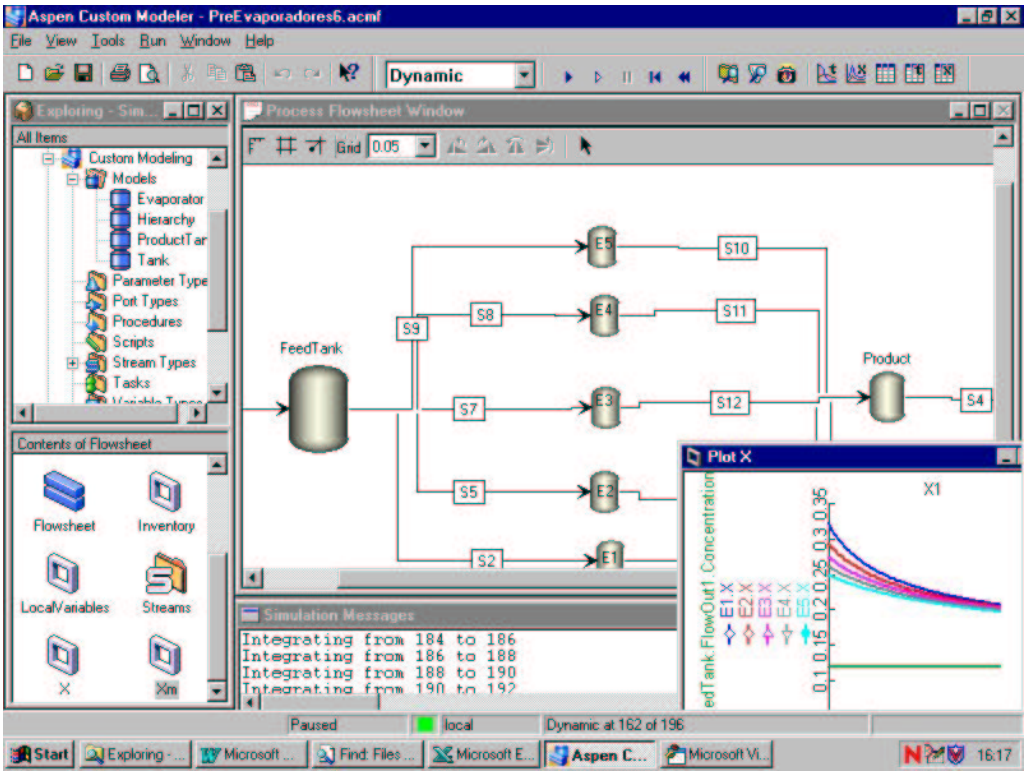

Figure 5.19: Screen-shot of the dynamic simulation

5.3.4 The simulation

As a final comment, the proposed RTE methodology has been programmed in Visual Basic, along with a graphical user interface (GUI) to follow the system execution, for validation purposes. Such program receives and sends information from and to a simulation case that emulates the plant. The simulation model is developed using Aspen Custom Modeler because switching between cleaning and operating modes is greatly facilitated using an adequate hybrid discrete-continuous process simulator (further details will be given in the section 6.3.2 of the next chapter).

The dynamic simulation model is composed of four basic blocks:

1. The **feed tank**: only includes the mass balance equations:

$$\frac{dM}{dt} = F_T - \sum_{j=1}^{p} F_{0,j} \tag{5.46}$$

2. The **evaporator** (evaporation line): where the evaporator (evaporation line) object is defined. It contains its variables types and equations. It has defined two states: operating and cleaning. The operating mode contains the differential form of equations that gives the

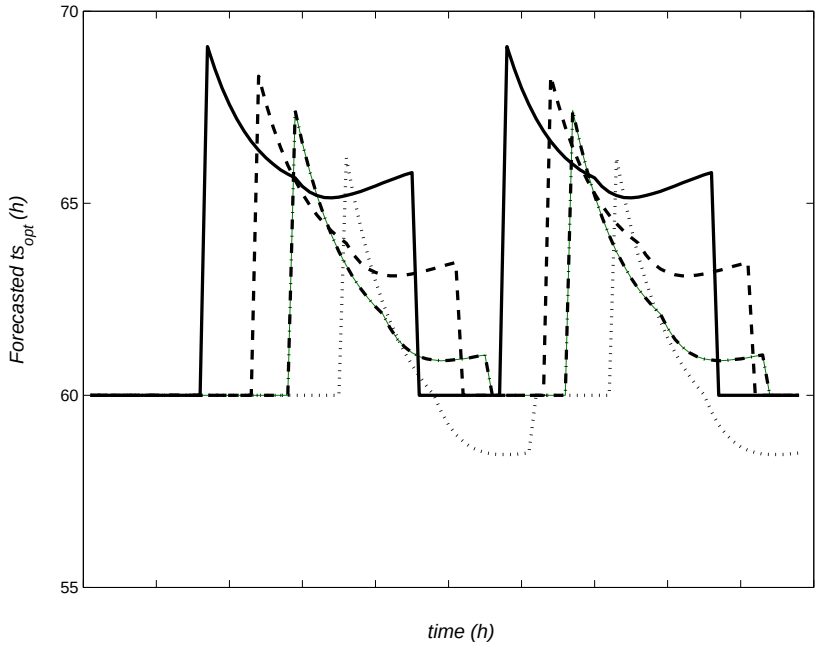

Figure 5.20: Continuous forecasting of optimal sub-cycle lengths obtained by the RT system over the dynamic simulation

outputs of the evaporator or line (according to the case), while during the cleaning mode there is no production.

3. The **product tank**: similarly to the feed tank, only contains the associated mass balance equations.

$$F_{P_T} = \sum_{j=1}^{p} F_{P_{n,j}} \tag{5.47}$$

$$F_{P_T} X_{m_T} = \sum_{j=1}^{p} F_{P_{n,j}} X_{m_{n,j}} \tag{5.48}$$

4. The **port**: that allows to streams carrying information about the flow and concentration between blocks.

The RTE module continuously obtains the plant (simulator) status and acts in consequence (start a cleaning action) when required. Besides, following the proposed procedure (algorithm 3) the forecasted values for ts_{opt_j} are obtained continuously, as is shown in figure 5.20.

5.3.5 Conclusions for the case study II

This subsection summarises the results obtained when applying the on-line/off-line methodology for the scheduling of processes with decaying performance developed in chapter 4 to an industrial case. In first place, although the proposed mathematical model is rather simple, a significant

improvement is achieved as compared with a simple rule of thumb approach. Furthermore, it results significantly more efficient than an alternative formulation. Besides the on-line approach provides the means for obtaining extra improvement that is of particular importance given the presence of model mismatch and variability for this case.

The RTE strategy has proved to obtain optimal solutions by using properly the information coming from the plant and answering simple questions on line, rather than performing successive formal optimisation, which has been the commonly used strategy.

5.4 Final comments about industrial case studies

The concepts developed in chapters 3 and 4 although already validated using simple benchmarks, have shown very satisfactory results when applied to these industrial problems. Not only they are perfectly applicable, but also, they have demonstrated again many advantages as compared to other approaches. In addition, it is important to mention that similar procedures to the used in this chapter for validating the approaches are a mandatory step prior the implementation. They are of major importance because they not only provide direct ways for increasing benefits (those related to the implementation) but also indirect ones since they also allow gaining better understanding of the process, its associated trade-offs, greatly helping in de-bottlenecking tasks.